

# Zeros of Partial Sums of the Riemann Zeta Function

Peter Borwein, Greg Fee, Ron Ferguson, and Alexa van der Waall

## CONTENTS

- 1. Introduction
- 2. Background
- 3. Zeros of Partial Sums
- 4. Zeros of Small Sums
- 5. Further Work
- Acknowledgments
- References

---

The semiperiodic behavior of the zeta function  $\zeta(s)$  and its partial sums  $\zeta_N(s)$  as a function of the imaginary coordinate has been long established. In fact, the zeros of a  $\zeta_N(s)$ , when reduced into imaginary periods derived from primes less than or equal to  $N$ , establish regular patterns. We show that these zeros can be embedded as a dense set in the period of a surface in  $\mathbb{R}^{k+1}$ , where  $k$  is the number of primes in the expansion. This enables us, for example, to establish the lower bound for the real parts of zeros of  $\zeta_N(s)$  for prime  $N$  and justifies the use of methods of calculus to find expressions for the bounding curves for sets of reduced zeros in  $\mathbb{C}$ .

---

## 1. INTRODUCTION

Figure 1 is a picture of the first 10,000 suitably normalized zeros of the fifth partial sum of the Riemann zeta function. (Precise definitions are given in later sections.)

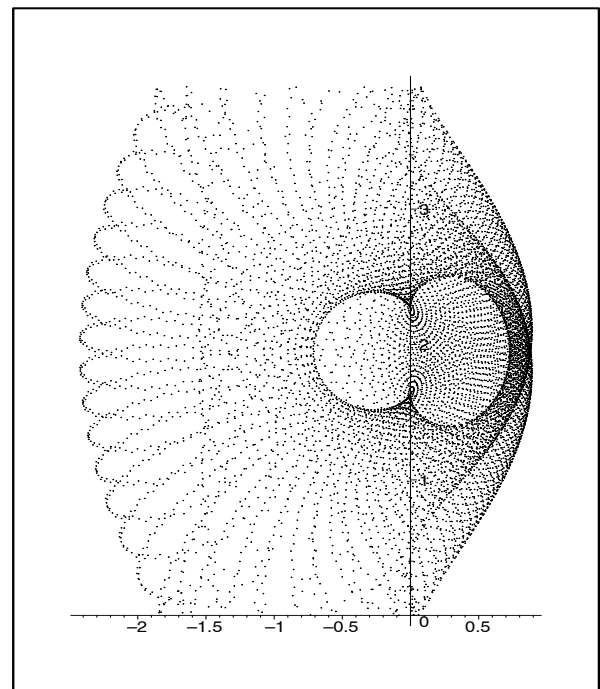


FIGURE 1. 10,000 normalized zeros of  $\zeta_5(s)$ .

2000 AMS Subject Classification: Primary 11M26;  
Secondary 11M41, 11Y35, 40A25

Keywords: Zeta function, Dirichlet series, zeros of exponential sums, series convergence

The picture is compelling—it suggests a phenomenon in need of an explanation—and this is indeed part of both the genesis and the purpose of this paper.

A second part of the genesis of the paper is a project to write a robust zero finder, in Maple, for virtually any analytic function on virtually any region. This is a hard problem, which will be discussed elsewhere. Finding a few zeros is easy; reliably finding all zeros is much harder. Even special-purpose figures, like those in this paper, require some effort to produce. Off-the-shelf software will probably not suffice.

Of course, any number theorist will first apply these methods to the Riemann zeta function in the hope of shedding a little more light on what number theorists certainly believe to be the most important unsolved problem in mathematics.

Section 2 gives a brief introduction to the Riemann zeta function. For a more comprehensive treatment the recent publication [Conrey 03] is recommended.

Section 3 discusses previous results for partial sums. Figure 2, made possible by our zero finder, indicates that even though the partial sums of  $\zeta_N(s)$  do not converge for  $\Re(s) \leq 1$ , there is some range in the complex plane where the zeros of the partial sum do approximate the zeros of  $\zeta(s)$ . Figure 3 gives a clearer indication that zeros of partial sums of the alternating series  $\eta(s)$  converge to zeros of the function itself. Theorem 3.1 improves previously published results on upper and lower bounds for the real parts of zeros of partial sums for  $\zeta(s)$  and  $\eta(s)$ . Refining this, in Theorem 4.10 we obtain a precise lower bound on the real parts of zeros of  $\zeta_N(s)$  for  $N$  prime.

Since  $\zeta(s)$  encodes so much information about prime numbers, it is natural to expect that a study of zeros of a partial sum will involve some study of the prime numbers involved in the sum. The first part of Section 4 studies the cases in which two primes are involved. The zeros of  $\zeta_3(s)$  are shown to be intersection points of two periodic functions, with periods  $2\pi i/\log(2)$  and  $2\pi i/\log(3)$ . A careful analysis shows precisely which intersection points are zeros of  $\zeta_3$  and their density as a function of  $\Im(s)$ . Theorem 4.5 gives a more general result for finite exponential sums involving only two primes, stating that all zeros lie on a periodic curve, where the number of choices for this period is infinite.

The second part of Section 4 is an extension to the case in which more primes are involved. The main result is Theorem 4.9, which shows how the discrete zeros of a finite exponential sum can be related to the zeros of a multiply periodic function. In particular, precise bounds

for the distribution of these zeros may be determined using methods of calculus.

## 2. BACKGROUND

Early studies of the function

$$\zeta(s) = \sum_{n=1}^{\infty} \frac{1}{n^s}, \quad s \in \mathbb{C}, \quad (2-1)$$

concerned its behavior for real  $s$ . Euler pointed out that this has a representation as a product

$$\zeta(s) = \prod_{p \text{ prime}} \left(1 - \frac{1}{p^s}\right)^{-1},$$

valid for  $s \in \mathbb{C}$  with  $\Re(s) > 1$ , first giving a hint of its importance in the study of prime numbers. It was Riemann, however, who, in his fundamental paper of 1859, outlined the analytic properties of what is now known as the *Riemann zeta function*. Writing  $s$  in the standard form

$$s = \sigma + it,$$

where  $\sigma$  and  $t$  are the real and imaginary parts of  $s$ , respectively, it is easily seen that the above series converges absolutely for  $\sigma > 1$ . Riemann showed that  $\zeta(s)$  has an analytic extension to a meromorphic function on  $\mathbb{C}$  having a single simple pole at  $s = 1$ . Moreover, he proved the surprising functional equation

$$\xi(s) := \frac{1}{2}s(s-1)\pi^{-s/2}\Gamma\left(\frac{s}{2}\right)\zeta(s) = \xi(1-s),$$

where  $\Gamma(s)$  is the usual gamma function. Using Euler's product formula, we derive that  $\zeta(s)$  has no zeros for  $\sigma > 1$ . The functional equation then shows that the only zeros of  $\zeta(s)$  in the left half-plane  $\sigma < 0$  coincide with the poles of  $\Gamma(s/2)$ , the so-called *trivial zeros* at  $s = -2, -4, -6, \dots$ . All other zeros must lie in the *critical strip*  $0 \leq \sigma \leq 1$ . Riemann asserted furthermore that the number of these roots whose imaginary parts are between 0 and  $T > 0$  is approximately

$$\frac{T}{2\pi} \log\left(\frac{T}{2\pi}\right) - \frac{T}{2\pi}, \quad (2-2)$$

with relative error term  $O(1/T)$ . Riemann stated that the same estimate should hold for all roots with real parts  $\frac{1}{2}$ , leading to the stronger conjecture that all roots of the zeta function in the critical strip lie on the *critical line*  $\sigma = \frac{1}{2}$ , the famous *Riemann hypothesis*. In 1905 von Mangoldt proved that the estimate (2-2) is correct,

with an error estimate of  $O(\log(T))$ ; see [Titchmarsh 86, Chapter 9].

The complex line  $\{z \in \mathbb{C} : \Re(s) = \frac{1}{2}\}$  is known as the *critical line*. The Riemann hypothesis was one of the 23 problems proposed by Hilbert in 1900 for mathematicians to work on in the twentieth century. It remains a problem for mathematicians in the twenty-first. It is known that there are at least  $KT \log(T)$  such zeros for some constant  $K > 0$  as  $T$  tends to  $\infty$ ; see [Titchmarsh 86, Section 10.9] or [Edwards 01]. Also, Conrey [Conrey 89] proved that more than 40% of the zeros of the Riemann zeta function are on the critical line. Through recent computations, X. Gourdon and P. Demichel claim confirmation that the first 10 trillion zeros with  $t > 0$  are indeed on the critical line.<sup>1</sup>

### 3. ZEROS OF PARTIAL SUMS

Since the series (2-1) does not converge for  $\sigma \leq 1$ , it is difficult to picture what relationship, if any, might exist between the zeros of the *truncated zeta function*

$$\zeta_N(s) := \sum_{n=1}^N \frac{1}{n^s}$$

and  $\zeta(s)$  in this half-plane. Figure 2, made possible through the application of the zero finder, illustrates a few points.

What is first noticeable is a string of zeros of  $\zeta_{211}$  near the critical line  $\sigma = \frac{1}{2}$ . Spira remarks in [Spira 66, Section 4] that the Euler–MacLaurin formulation

$$\begin{aligned} \zeta(s) &= \zeta_{N-1}(s) + N^{-s} + \frac{N^{1-s}}{s-1} \\ &+ \sum_{n=1}^k \frac{B_{2n}}{(2n)!} \left( \prod_{j=0}^{2n-2} (s+j) \right) N^{1-s-2n} + R(k, n, s), \end{aligned}$$

where

$$\begin{aligned} R(k, N, s) &< \left| \frac{B_{2(k+1)}}{(2(k+1))!} \left( \prod_{j=0}^{2k} (s+j) \right) N^{1-s-2(k+1)} \right| \\ &\times \frac{|s+2k+1|}{|\sigma+2k+1|}, \end{aligned}$$

implies that  $\zeta(s)$  is roughly approximated by  $\zeta_N(s)$  near the critical line for  $t < 2\pi N$ , but  $t$  also large enough so that  $N^{1/2}/t$  is “small.” The strip of zeros is in accordance with Spira’s observation. Above  $t = 2\pi N$ , about 1326 in Figure 2, the zeros scatter more wildly.

<sup>1</sup><http://numbers.computation.free.fr/Constants/Miscellaneous/zetazeroscompute.html>.

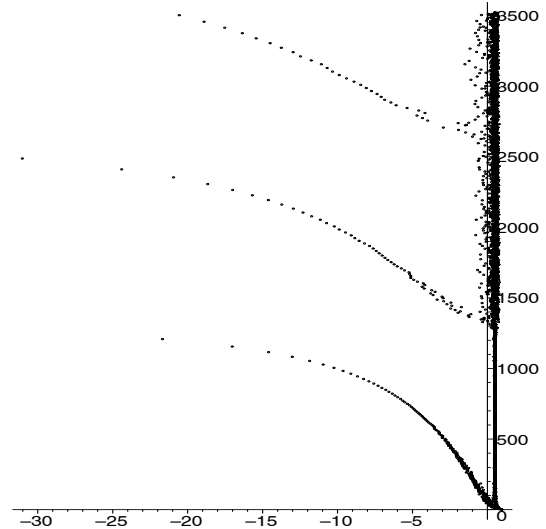


FIGURE 2. 3000 zeros of  $\zeta_{211}(s)$ .

In [Turán 48], Turán points to a possible relationship between the behavior of the roots of the partial sums of the zeta function (2-1) and the Riemann hypothesis. He proves in his Theorem II that the Riemann hypothesis is valid if there are positive numbers  $n_0$  and  $K$  such that for  $N > n_0$  the truncated zeta function  $\zeta_N(s)$  does not vanish in the half-plane

$$\sigma \geq 1 + \frac{K}{\sqrt{N}}.$$

In [Montgomery 83], however, Montgomery shows that for given  $0 < c < \frac{4}{\pi} - 1$  and for  $N$  large enough the function  $\zeta_N$  always has zeros in the half-plane

$$\sigma > 1 + c \frac{\log \log(N)}{\log(N)},$$

making Turán’s theorem vacuous. Still, it is interesting that connections can be made between zeros of  $\zeta(s)$  in the critical strip and zeros of the partial sums  $\zeta_N(s)$ .

Striking in Figure 2 are the three strings of zeros trailing to the left, both above and below the string of zeros near the critical line. The bottom string originates in a region near  $s = 1$  where the zeros are fairly scattered. A result of Knopp [Jentzsch 18, p. 236] asserts that every point of  $\sigma = 1$ , the line of convergence for the  $\zeta$  series, is an accumulation point of the zeros of the partial sums  $\zeta_N$ . As  $N$  increases, we expect such patterns to continue, with the lower string in particular moving upward on the left and becoming steeper and moving closer to the line  $\sigma = 1$  on the right.

The comparison with partial sums in the critical strip is more direct for the *alternating zeta function*, defined

by

$$\eta(s) := \sum_{n=1}^{\infty} (-1)^{n+1} \frac{1}{n^s},$$

in its region of convergence  $\sigma > 0$  and then extended by analytic continuation. We derive that

$$\eta(s) = \left(1 - \frac{2}{2^s}\right) \zeta(s),$$

so all the zeros of  $\zeta(s)$  are zeros of  $\eta(s)$ . In particular,  $\zeta(s)$  and  $\eta(s)$  have the same zeros within the critical strip. As well,  $\eta(s)$  has the zeros of  $1 - 2^{1-s}$ , namely, the points

$$\omega_k := 1 + \frac{2k\pi i}{\log(2)}, \quad k \in \mathbb{Z}. \quad (3-1)$$

The *truncated alternating zeta functions*

$$\eta_N(s) := \sum_{n=1}^N (-1)^{n+1} \frac{1}{n^s}, \quad N \in \mathbb{Z}_{>0},$$

converge in the plane  $\sigma > 0$  to the alternating zeta function as  $N$  tends to  $\infty$ . In particular, they have roots “close” to the  $\omega_k$ ’s if  $N$  is sufficiently large. More specifically, the point

$$\omega_k + \frac{1}{4 \log(2) \cdot \zeta(\omega_k)} (N + 1)^{-2+\omega_k}$$

is the asymptotic expression of a root of  $\eta_{2N}$  that converges to  $\omega_k$  for  $N \rightarrow \infty$ ; see [Turán 48, Section 7].

Consider now Figure 3. Above  $t = 0$ , we see two strings of zeros, one close to the critical line approximating the zeros of the zeta function, and the other close to

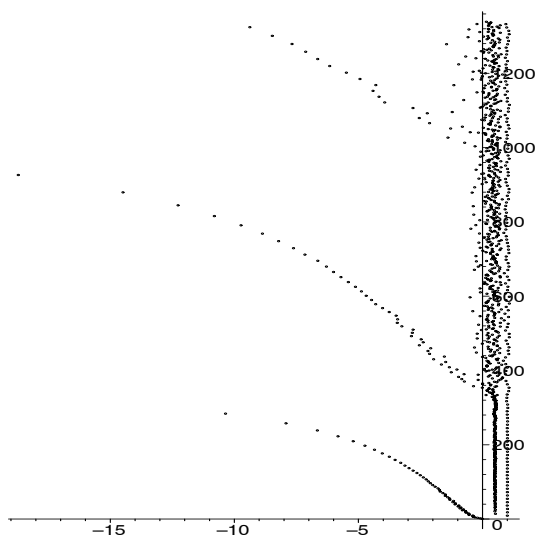


FIGURE 3. 1000 zeros of  $\eta_{109}(s)$ .

$s = 1$  approximating the zeros of  $1 - 2^{1-s}$ , as expected. Above these the zeros scatter more wildly, as in Figure 2.

It has been proved in the papers [Langer 31] and [Wilder 17] that the number  $M$  of zeros of  $\zeta_N$  in the upper half-plane that have imaginary part less than  $T$  satisfies

$$\left| M - \left\lfloor \frac{\log(N)T}{2\pi} \right\rfloor \right| \leq N. \quad (3-2)$$

This approximates the density of the zeros of  $1 \pm 1/N^s$ , which occur one every distance of  $2\pi/\log(N)$  up the imaginary axis, or a frequency of  $\log(N)/2\pi$ .

Using (2-2) and (3-1), we see that the number of roots of  $\eta(s)$  in the same region has the estimate

$$\frac{T}{2\pi} \log\left(\frac{T}{2\pi}\right) - \frac{T}{2\pi} + \frac{(\log(2))T}{2\pi}.$$

Differentiating with respect to  $T$ , we obtain a frequency of  $\log(T/\pi)/2\pi$  for these roots as we move up the imaginary axis. These two frequencies match at  $T = N\pi$ , which for Figure 3 evaluates as  $342.4\dots$ , approximately where this scattering begins. Above this, the number of zeros of the partial sum is insufficient to match those of  $\eta(s)$ , while below they are in excess, giving some explanation for the string of zeros trailing to the left at the bottom.

The alternating series converges for  $\sigma > 0$ . The complete set of accumulation points of zeros of the truncated alternating zeta functions  $\eta_N$  consists of the line  $\sigma = 0$ , the roots of  $\zeta(s)$ , and the zeros  $\omega_k$ ; see [Turán 48, Section 7]. We therefore anticipate the line of convergence,  $\sigma = 0$  in this case, to be the set of limit points of these bottom strings of zeros and their conjugates as  $N$  increases.

Turán showed [Turán 59] that the positions of zeros in the half-plane  $\sigma > 1$  for the partial sums of the alternating zeta function also has relevance for the Riemann hypothesis. Though his estimates in this case as well were proved redundant by Montgomery’s work, it is interesting to obtain actual bounds for the real values of these roots.

It is proved in [Spira 66] that all zeros of  $\zeta_N$  have real parts

$$1 - N < \sigma < 1.85.$$

The following simple argument improves this.

**Theorem 3.1.** *Let  $s$  be a zero of  $\zeta_N$  or  $\eta_N$ . Then  $s$  satisfies  $\sigma \leq \alpha$ , where  $\alpha$  is the positive root of  $\zeta(\sigma) = 2$ . In particular, one has  $\sigma < 1.73$ .*

*Also,  $s$  satisfies  $\sigma \geq \beta_N$ , where  $\beta_N$  is the negative root of  $\zeta_{N-1}(\sigma) = N^{-\sigma}$ .*

*Proof:* Let  $s$  be a zero of  $\zeta_N$  such that  $\sigma > 1$ . Then

$$\begin{aligned} 1 &= | -2^{-s} - 3^{-s} - \dots - N^{-s} | \\ &\leq 2^{-\sigma} + 3^{-\sigma} + \dots + N^{-\sigma} \\ &\leq \zeta(\sigma) - 1. \end{aligned}$$

Since the functions in these inequalities are positive and decreasing in  $\sigma$ , we need to find the positive solution of  $\zeta(s) = 2$ . This is  $s = 1.728647239$ .

Similarly,

$$\begin{aligned} |N^{-s}| &= N^{-\sigma} = |1 + 2^{-s} + 3^{-s} + \dots + (N - 1)^{-s}| \\ &\leq 1 + 2^{-\sigma} + 3^{-\sigma} + \dots + (N - 1)^{-\sigma}. \end{aligned}$$

The equation  $N^{-\sigma} = \zeta_{N-1}(\sigma)$  is equivalent to  $N^\sigma \zeta_{N-1}(\sigma) = 1$ . Note that  $N^\sigma \zeta_{N-1}(\sigma)$  is an increasing function of  $\sigma$ , with asymptote 0 as  $\sigma \rightarrow -\infty$  and value  $N - 1$  at 0. Thus  $N^{-\sigma} = \zeta_{N-1}(\sigma)$  has a single negative root,  $\sigma = \beta_N$ . For  $\sigma < \beta_N$  the above inequality no longer holds. These proofs hold in the same way for the zeros of  $\eta_N$ .  $\square$

For  $\zeta_N(s)$ , Turán shows in [Turán 48, Theorem IV] that for  $N$  large enough,  $\zeta_N(s) \neq 0$  for

$$\sigma \geq 1 + 2(\log \log N) / \log(N),$$

so an improved upper bound should be possible in this case. However, the lower bound is closer to the truth. Indeed, for  $N$  prime, we show in Theorem 4.10 below that this is the actual bound.

An easy argument shows that  $\beta_N = -(N + o(N)) \log(2)$ . Writing  $\beta_N = b_N N$ , we have

$$\begin{aligned} N^{b_N N} + \dots + \left( \left( 1 - \frac{2}{N} \right)^N \right)^{-b_N} + \left( \left( 1 - \frac{1}{N} \right)^N \right)^{-b_N} \\ = 1. \end{aligned}$$

We note that  $\lim_{N \rightarrow \infty} \left( 1 - \frac{k}{N} \right)^N = e^{-k}$ . A limit  $b_N \rightarrow b_\infty$  would imply

$$1 \approx e^{b_\infty} + e^{2b_\infty} + e^{3b_\infty} + \dots,$$

giving  $b_\infty = -\log(2)$  as a first approximation. Computationally, the estimate  $\beta_N \approx -(N - 3/2) \log(2)$  holds with surprising accuracy at  $N = 5$  and with increasing accuracy to at least  $N = 100,000$ .

#### 4. ZEROS OF SMALL SUMS

##### 4.1 Single-Parameter Curves

Figure 4 shows the positions in the upper half-plane of the first 2000 zeros of

$$\zeta_3(s) = 1 + \frac{1}{2^s} + \frac{1}{3^s}.$$

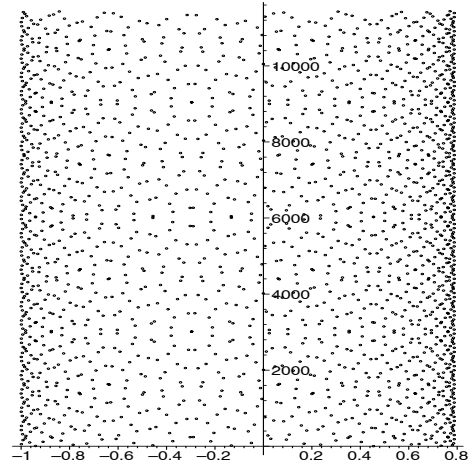


FIGURE 4. The first 2000 zeros of  $\zeta_3(s)$ .

Although the zeros are not recurring in a completely regular pattern, their positioning does appear to have a semi-periodic nature. The algorithm used to locate these zeros uses a homotopy. In its more general form, for  $\zeta_N$ , starting from the known position of the zeros of the end terms

$$1 + \frac{1}{N^s},$$

at the points  $\{2\pi ki / \log(N) : k \in \mathbb{N}\}$ , Newton's method was used to find zeros along the path

$$1 + \frac{1}{N^s} + t \left( \sum_{n=2}^{N-1} \frac{1}{n^s} \right)$$

as  $t$  increased from 0 to 1. That this method worked so well in locating all of the zeros of  $\zeta_N(s)$  up to heights tested suggests that the error estimate in (3-2) above could be improved to  $O(1)$ . In any case, in such finite exponential sums, the largest integer in the expansion,  $N$ , is an indicator of the number of zeros to be found up to a height  $T$  in much the same way as the degree of a polynomial determines its number of zeros in the complex plane.

It is then natural to plot the difference between the zeros found for  $\zeta_N$  and the starting values of each path. This was the inspiration for the plot on the left of Figure 5, where the imaginary parts of the zeros are reduced modulo  $2\pi / \log(3)$ , the distance between zeros of  $1 + 1/3^s$ .

We now see a striking regularity. An explanation is fairly simple. The equation  $\zeta_3(s) = 0$  becomes two equations in the real and imaginary parts:

$$1 + 2^{-x} \cos(\log(2)y) + 3^{-x} \cos(\log(3)y) = 0, \quad (4-1)$$

$$2^{-x} \sin(\log(2)y) + 3^{-x} \sin(\log(3)y) = 0, \quad (4-2)$$

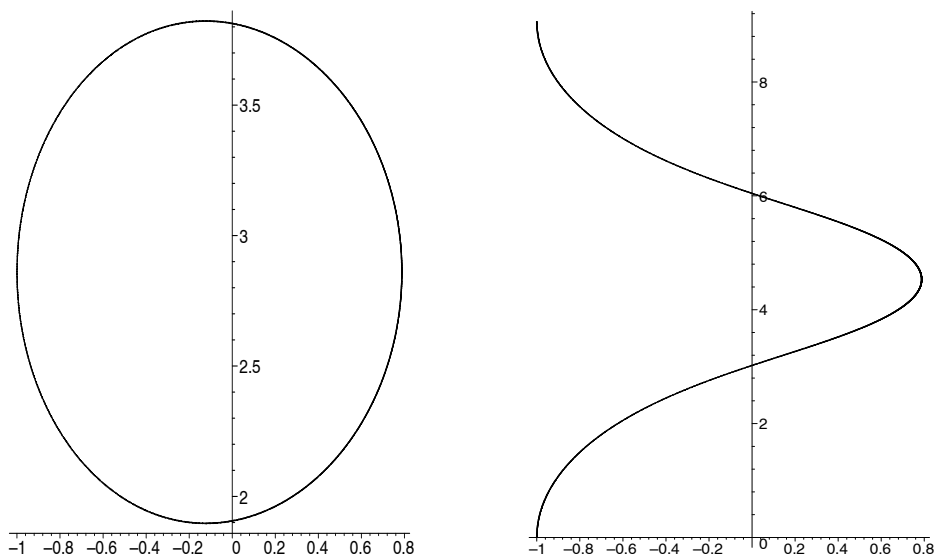


FIGURE 5. Zeros of  $\zeta_3(s)$  reduced modulo  $\frac{2\pi i}{\log(3)}$  and  $\frac{2\pi i}{\log(2)}$ .

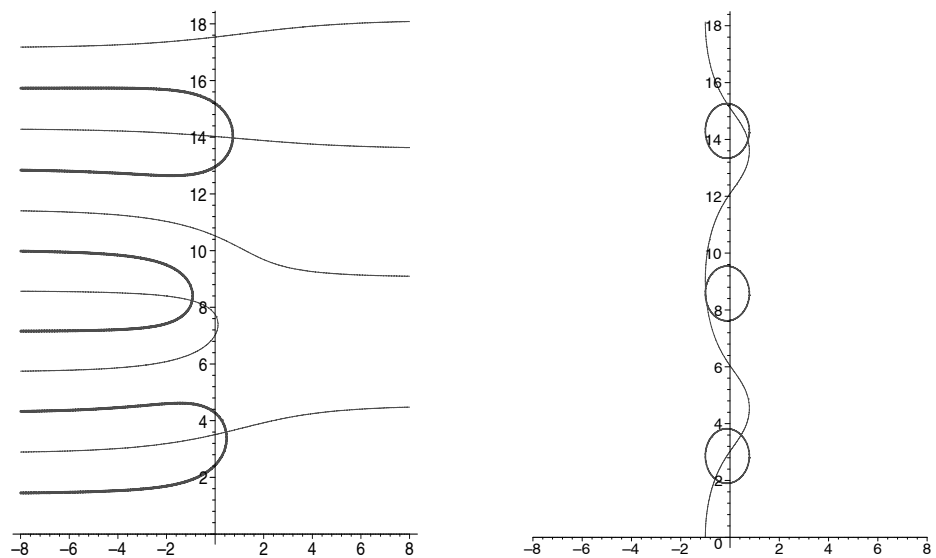


FIGURE 6. Comparison of intersection points.

where  $s = x + iy$ . Using the trigonometric formula  $\cos^2(\log(2)y) + \sin^2(\log(2)y) = 1$ , we derive

$$1 + 2 \cdot 3^{-x} \cos(\log(3)y) + 9^{-x} = 4^{-x}. \tag{4-3}$$

This is a curve with period  $2\pi/\log(3)$  in  $y$  that must contain all the zeros of  $\zeta_3(s)$ . If we reduce the imaginary parts of the zeros modulo  $2\pi/\log(3)$ , they still lie on the same curve, but all within a single period.

The same procedure may be applied to remove terms in  $\log(3)y$ , giving

$$1 + 2 \cdot 2^{-x} \cos(\log(2)y) + 4^{-x} = 9^{-x}. \tag{4-4}$$

Zeros reduced modulo  $2\pi/\log(2)$  lie on a period of this curve, as shown on the right of Figure 5.

We can use the curves (4-3) and (4-4) to obtain a good description of the zeros of  $\zeta_3(s)$ . Figure 6 allows us to compare intersection points.

The graph on the left shows intersection points of the curves  $\Re(\zeta_3(s)) = 0$  and  $\Im(\zeta_3(s)) = 0$  as given in (4-1) and (4-2) above, these points being zeros of  $\zeta_3(s)$ . The graph on the right shows intersection points of the curves (4-3) and (4-4). These points include the zeros of  $\zeta_3(s)$ , but as we can see in the comparison, not all of the inter-

section points are zeros of  $\zeta_3(s)$ . This graph does show that the real parts of these zeros are bounded, something now evident from the graph on the left.

A more careful analysis is needed to show which intersection points of (4-3) and (4-4) are zeros of  $\zeta_3(s)$  and to describe their distribution.

**Lemma 4.1.** *The zeros of  $\zeta_3(s)$  are those points satisfying Equations (4-3) and (4-4) for which  $\sin(\log(3)y)$  and  $\sin(\log(2)y)$  are of opposite signs.*

*Proof:* Any zero of  $\zeta_3(s)$  must satisfy (4-3) and (4-4), since they are derived from (4-1) and (4-2).

Conversely, we obtain (4-1) by adding (4-3) and (4-4). From Equation (4-3), we obtain

$$\begin{aligned} |\sin(\log(3)y)| &= (1 - \cos^2(\log(3)y))^{1/2} \\ &= \frac{(4 \cdot 9^{-x} - (4^{-x} - 9^{-x} - 1)^2)^{1/2}}{2 \cdot 3^{-x}} \\ &= \frac{((4^{-x} - (3^{-x} - 1)^2)((3^{-x} + 1)^2 - 4^{-x}))^{1/2}}{2 \cdot 3^{-x}}. \end{aligned}$$

Similarly, from (4-4), we obtain

$$\begin{aligned} |\sin(\log(2)y)| &= \frac{((9^{-x} - (2^{-x} - 1)^2)((2^{-x} + 1)^2 - 9^{-x}))^{1/2}}{2 \cdot 2^{-x}} \\ &= \frac{3^{-x}}{2^{-x}} |\sin(\log(3)y)|. \end{aligned}$$

Thus, (4-2) is satisfied if  $\sin(\log(3)y)$  and  $\sin(\log(2)y)$  are of opposite signs.  $\square$

This gives us an easy method for deciding which intersections of the curves (4-3) and (4-4) are actual zeros of  $\zeta_3(s)$ . We now need a better description of these curves.

**Lemma 4.2.**

(1) *The curve given by Equation (4-3) consists of congruent convex, closed curve segments contained in and tangent at each edge of the disjoint boxes*

$$[-1, r_1] \times \left[ \frac{(2k+1)\pi}{\log(3)} - r_2, \frac{(2k+1)\pi}{\log(3)} + r_2 \right],$$

where  $k \in \mathbb{Z}$ ,  $r_1$  is the real root of  $1 - 2^{-x} - 3^{-x} = 0$ , and  $r_2$  is the point where the derivative of  $(\frac{3}{4})^x - 3^x - 1/3^x$  is 0.

(2) *The curve given by Equation (4-4) is single-valued in  $x$ , with maximum  $x$ -values obtained at the points*

$$\left( r_1, \frac{(2k+1)\pi}{\log(2)} \right)$$

and minimum  $x$ -values at the points

$$\left( -1, \frac{2k\pi}{\log(2)} \right)$$

for  $k \in \mathbb{Z}$ . It has positive slope in the half-periods

$$y \in \left[ \frac{2k\pi}{\log(2)}, \frac{(2k+1)\pi}{\log(2)} \right]$$

and negative slope in the half-periods

$$y \in \left[ \frac{(2k-1)\pi}{\log(2)}, \frac{2k\pi}{\log(2)} \right]$$

for  $k \in \mathbb{Z}$ .

*Proof:* (1) We start by rewriting Equation (4-3) as

$$\cos(\log(3)y) = \frac{1}{2} \left( \left( \frac{3}{4} \right)^x - 3^x - \frac{1}{3^x} \right)$$

and analyzing the function

$$\begin{aligned} f(x) &:= \frac{1}{2} \left( \left( \frac{3}{4} \right)^x - 3^x - \frac{1}{3^x} \right) \\ &= \frac{1}{2} \left( \frac{3}{4} \right)^x - \cosh((\log(3))x) \end{aligned}$$

on the right. For  $x > 0$  the term  $-3^x$  dominates, while for  $x < 0$  the term  $-1/3^x$  dominates, so  $f(x) \rightarrow -\infty$  as  $x \rightarrow \pm\infty$ . Its derivative

$$f'(x) = -\frac{1}{2} \log\left(\frac{4}{3}\right) \left(\frac{3}{4}\right)^x - \log(3) \sinh((\log(3))x)$$

is the sum of two decreasing functions and so is decreasing, having a single zero at  $r_2 = -0.1230\dots$  with  $f(r_2) = -0.4911\dots$ . Thus,  $f(x)$  increases up to  $r_2$  and then decreases. The curve is defined only where  $\cos(\log(3)y) \leq f(r_2)$ , i.e., in regions where

$$\frac{(2k+1)\pi - y_1}{\log(3)} \leq y \leq \frac{(2k+1)\pi + y_1}{\log(3)}$$

with  $y_1 = \pi - \arccos(f(r_2)) = 1.0574\dots < \pi/2$ . For each  $y$ -value in the interval

$$\left( \frac{(2k+1)\pi - y_1}{\log(3)}, \frac{(2k+1)\pi + y_1}{\log(3)} \right)$$

there are two solutions in  $x$ , so that the curve decomposes into disjoint closed paths. The curve achieves its extreme values in  $x$  at the points  $y = \frac{(2k+1)\pi}{\log(3)}$  where  $\cos(\log(3)y) = -1$ , giving

$$0 = f(x) + 1 = -\frac{3^x}{2} \left( 1 + \frac{1}{2^x} - \frac{1}{3^x} \right) \left( 1 - \frac{1}{2^x} - \frac{1}{3^x} \right).$$

A simple analysis shows that this has only two real roots,  $-1$  and  $r_1$ .

For the curve, we have

$$(\log(3)) \sin((\log(3))y) \frac{dy}{dx} = -f'(x).$$

At the extreme values for  $x$ , we have  $\sin((\log(3))y) = 0$ , making the tangents vertical. At the points on the curve with  $x = r_2$ , we have  $f'(x) = 0$ , making the tangents horizontal.

The closed paths are symmetric about the lines  $y = (2k + 1)\pi/\log(3)$ . For  $y \in [(2k + 1)\pi - y_1]/\log(3), (2k + 1)\pi/\log(3)]$ , we have  $\sin((\log(3))y) > 0$ , so that the curve is strictly decreasing for  $x \in (-1, r_2)$  and strictly increasing for  $x \in (r_2, r_1)$ .

To determine convexity, we evaluate the second derivative, obtaining

$$\begin{aligned} &(\log(3)) \sin((\log(3))y) \frac{d^2y}{dx^2} \\ &= (\log(3))^2 \frac{(3^x + 3^{-x})}{2} - \log\left(\frac{3}{4}\right)^2 \frac{\left(\frac{3}{4}\right)^x}{2} \\ &\quad - (\log(3))^2 \cos((\log(3))y) \left(\frac{dy}{dx}\right)^2. \end{aligned}$$

For

$$y \in [((2k + 1)\pi - y_1)/\log(3), (2k + 1)\pi/\log(3)]$$

we have

$$\sin((\log(3))y) > 0, \quad \cos((\log(3))y) < 0.$$

Also, for  $x > 0$ ,

$$(\log(3))^2 3^x - \log\left(\frac{3}{4}\right)^2 \frac{\left(\frac{3}{4}\right)^x}{2} > 0,$$

and for  $x < 0$ ,

$$(\log(3))^2 3^{-x} - \log\left(\frac{3}{4}\right)^2 \frac{\left(\frac{3}{4}\right)^x}{2} > 0.$$

Thus,  $\frac{d^2y}{dx^2} > 0$ , and the portions of the curve for these  $y$ -values are convex up. Using symmetry, we obtain that the regions enclosed by the closed paths are convex.

(2) Curve (4-3) is easier to analyze. In this case, let

$$f(x) = \frac{\left(\frac{2}{9}\right)^x - (2^x + 2^{-x})}{2}.$$

Then the curve has the equivalent formulation

$$\cos((\log(2))y) = f(x).$$

For  $x < 0$ , the term  $\left(\frac{2}{9}\right)^x$  dominates, so  $\lim_{x \rightarrow -\infty} = \infty$ . For  $x > 0$ , the term  $2^x$  dominates, so  $\lim_{x \rightarrow \infty} = -\infty$ . We easily see that  $f(x)$  is a strictly decreasing function, since for  $x < 0$ , both  $(2/9)^x - 2^{-x}$  and  $-2^x$  are strictly decreasing, while for  $x > 0$  both  $(2/9)^x$  and  $-(2^x + 2^{-x})/2 = -\cosh((\log(2))x)$  are strictly decreasing and  $f'(0) = \log(2/9)/2 < 0$ . Thus, every  $y$ -value corresponds to a single  $x$ -value on the curve. Differentiating, we obtain

$$-\sin((\log(2))y) \frac{dy}{dx} = f'(x).$$

Since  $f'(x) < 0$  for all  $x$ , the sign of  $\frac{dy}{dx}$  is the same as the sign of  $\sin((\log(2))y)$ , giving the result as stated.  $\square$

We now have a theorem justifying the figures presented.

**Theorem 4.3.**

- (1) The zeros of  $\zeta_3(s)$  modulo  $2\pi i/\log(3)$  are dense in the curve  $1 + 2 \cdot 3^{-x} \cos(\log(3)y) + 9^{-x} = 4^{-x}$  over the period  $y \in [0, 2\pi/\log(3)]$ .
- (2) The zeros of  $\zeta_3(s)$  modulo  $2\pi i/\log(2)$  are dense in the curve  $1 + 2 \cdot 2^{-x} \cos(\log(2)y) + 4^{-x} = 9^{-x}$  over the period  $y \in [0, 2\pi/\log(2)]$ .
- (3) The real parts of the zeros of  $\zeta_3(s)$  are dense in the interval  $[-1, r_1]$ .

*Proof:* (1) This uses the facts that both curves (4-4) and (4-3) have the same range of  $x$ -values and that the periods  $[0, 2\pi/\log(3)]$  and  $[0, 2\pi/\log(2)]$  are rationally independent. For a point  $(x, y + 2k\pi/\log(3))$  on (4-4) in its first period, consider the point  $(x, y')$  on curve (4-3) in its first period such that  $\sin((\log(3))y)$  and  $\sin((\log(2))y')$  are of opposite signs. Then we can find  $0 < k, l \in \mathbb{Z}$  such that  $y + 2k\pi/\log(3)$  and  $y' + 2l\pi/\log(2)$  are arbitrarily close. Thus we can find intersection points  $(x_n, y_n)$  that are zeros of  $\zeta_3(s)$  such that  $x_n \rightarrow x$  and  $y_n \pmod{2\pi/\log(3)} \rightarrow y$ . Assertion (2) follows from a like argument, while (3) follows easily from either (1) or (2).  $\square$

*Note:* A more general result is given in Corollary 4.11 below.

**Theorem 4.4.** All of the zeros of  $\zeta_3(s)$  are simple. They are distributed so that each disjoint closed segment of the curve  $1 + 2 \cdot 3^{-x} \cos(\log(3)y) + 9^{-x} = 4^{-x}$  contains exactly one zero of  $\zeta_3(s)$ .

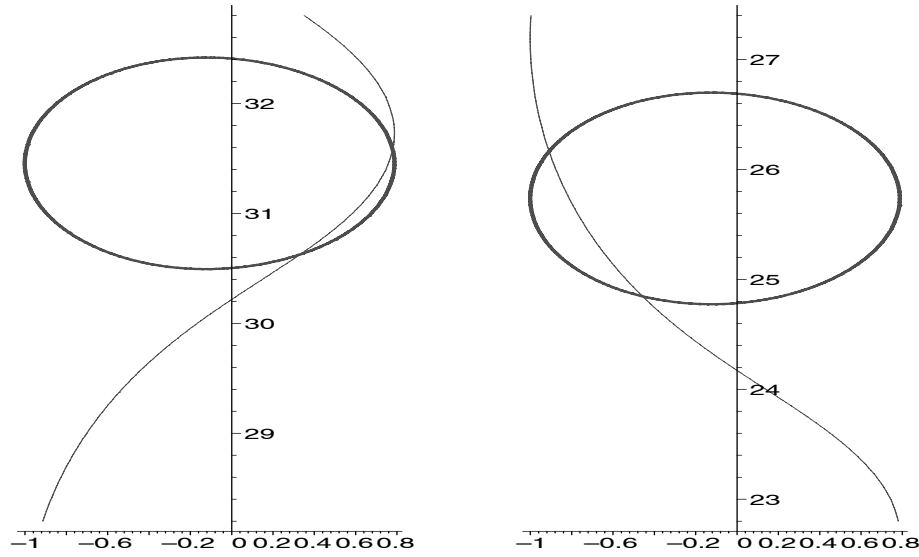


FIGURE 7. Intersections of curves (4-3) and (4-4).

*Proof:* If a zero of an analytic function

$$F(z) = f(x, y) + ig(x, y)$$

has multiple roots at  $z = a + ib$ , then

$$F'(a + ib) = \frac{\partial f}{\partial x}(a, b) + i \frac{\partial g}{\partial x}(a, b) = 0.$$

For  $\zeta_3(z)$  this translates to the conditions

$$\begin{aligned} (\log(2))2^{-x} \sin((\log(2))y) + (\log(3))3^{-x} \sin((\log(3))y) \\ = 0 \end{aligned} \quad (4-5)$$

and

$$\begin{aligned} (\log(2))2^{-x} \cos((\log(2))y) + (\log(3))3^{-x} \cos((\log(3))y) \\ = 0. \end{aligned} \quad (4-6)$$

From (4-5) and (4-2) we obtain  $\sin((\log(2))y) = \sin((\log(3))y) = 0$ , which is impossible since  $\log(2)$  and  $\log(3)$  are rationally independent. Therefore, all zeros of  $\zeta_3(s)$  must be simple.

For the second claim in the theorem, consider the two cases illustrated in Figure 7.

Both graphs show the intersection of curve (4-4) with a single closed segment of curve (4-3), where curve (4-4) enters from below with positive slope on the left and with negative slope on the right. We will show in each case that curve (4-4) has exactly two points of intersection with curve (4-3) and exits from above with the slope of the same sign as on entry. Thus,  $\sin((\log(2))y)$  keeps the same sign at the entry and exit points, while  $\sin((\log(3))y)$

changes, so that exactly one of these points is a zero of  $\zeta_3(s)$ .

Note first that points on each closed segment of curve (4-3) encompass the full range of  $x$ -values of curve (4-4). Thus, each closed segment of curve (4-3) must intersect curve (4-4). Both curves achieve their extreme  $x$ -values at  $y$ -values that are integer multiples of their half-periods, and therefore rationally independent. Thus, these cannot be intersection points for the curves, meaning that curve (4-4) must intersect at least once with the lower half and at least once with the upper half of each closed segment.

Consider the first case, in which the slope of curve (4-4) is positive, i.e., in one of its first half-periods. We show that wherever this curve intersects with curve (4-3) in one of its first half-periods, i.e., the lower half of one of the closed segments, the slope of curve (4-4) is strictly greater than that of curve (4-3). A second intersection before curve (4-3) achieves its maximum  $x$ -value is then impossible, since (4-4) would then have to cross (4-3) from left to right and have lower slope.

We rewrite Equations (4-3) and (4-4) as

$$\begin{aligned} 2 \cos(\log(3)y) &= (3/4)^x - 3^x - 1/3^x, \\ 2 \cos(\log(2)y) &= (2/9)^x - 2^x - 1/2^x. \end{aligned}$$

Differentiating, we obtain

$$\begin{aligned} 2(\log(3)) \sin((\log(3))y) \frac{dy}{dx} \\ = (3/4)^x \log(3/4) - (\log(3))(3^x - 1/3^x) \end{aligned}$$

and

$$2(\log(2)) \sin((\log(2))y) \frac{dy}{dx} = (2/9)^x \log(2/9) - (\log(2))(2^x - 1/2^x).$$

At intersection in the first half-periods of both curves we have

$$2^{-x} \sin((\log(2))y) = 3^{-x} \sin((\log(3))y),$$

so that the ratio of the slope of curve (4-3) to (4-4) simplifies to

$$R(x) = \frac{\log(2)}{\log(3)} \times \frac{\log(3)36^x - 9^x \log(3) + 2 \log(2)9^x - 4^x \log(3)}{\log(2)36^x - 4^x \log(2) + 2 \cdot 4^x \log(3) - \log(2)9^x}.$$

To show that  $R(x)$  is increasing over  $[-1, r_1]$ , we look at its derivative, which simplifies to

$$R'(x) = \frac{4 \log(2)}{\log(3)} \times \frac{36^x ((\log(3))^3 4^x - (\log(2))^3 9^x - (\log(3/2))^3)}{((\log(2))36^x - (\log(2))4^x + 2(\log(3))4^x - (\log(2))9^x)^2}.$$

The only factor that changes sign is

$$f(x) := ((\log(3))^3 4^x - (\log(2))^3 9^x - (\log(3/2))^3).$$

We see that  $f(x)$  approaches the horizontal asymptote  $y = -(\log(3/2))^3$  as  $x \rightarrow -\infty$  and has a single critical point where  $(9/4)^x = (\log(3)/\log(2))^2$  or  $x_c = 1.13588\dots$ . Thus,  $f(x)$  is increasing on  $[-\infty, x_c]$ . Since  $f(-1) = 0.2278\dots > 0$ , we have  $R'(x) > 0$  on  $[-1, r_1]$ , and hence  $R(x)$  increases on  $[-1, r_1]$ . We obtain  $R(-1) = -0.4206\dots$  and  $R(r_1) = 0.8684\dots$ , so  $|R(x)| < 1$  on  $[-1, r_1]$ . Since the slope of curve (4-4) is always positive in this consideration, we have that the slope of curve (4-4) is strictly greater than that of curve (4-3) at any point of intersection, as claimed.

In the second case shown in Figure 7, the slope of curve (4-3) is negative. Where it intersects with curve (4-4) in one of its first half-periods we have

$$2^{-x} \sin((\log(2))y) = 3^{-x} \sin((\log(3))y).$$

For the ratio of slopes,  $R(x)$  in this case, we again have  $|R(x)| < 1$ , meaning that the slope of curve (4-4) is strictly less than that of curve (4-3). Thus, there is only one intersection in this first half-period of curve (4-4).

By the symmetry of the cosine functions for  $y$ -values, curve (4-3) has a single intersection in each case with the

second half-periods of curve (4-4). These must be in the same half-periods of curve (4-3). For the two intersections in each case, the sign of  $\sin((\log(2))y)$  remains the same, while that of  $\sin((\log(3))y)$  changes. The theorem follows then, from Lemma 4.1.  $\square$

The occurrence of periods is expressed more generally in the following theorem.

**Theorem 4.5.** *Let  $\zeta_{N,p,q}(s)$  be an exponential sum composed of terms  $c_n/n^s$ , where  $c_n$  is constant and  $n$  is divisible only by the primes  $p$  and  $q$ . Then the zeros of  $\zeta_{N,p,q}(s)$  reduced modulo*

$$\left| \frac{2\pi i}{m_1 \log(p) + m_2 \log(q)} \right|$$

lie on a period of a curve, where  $(m_1, m_2) = (0, 1)$  or  $(1, 0)$  or  $m_1, m_2 \in \mathbb{Z}$  with  $\gcd(m_1, m_2) = 1$ .

*Proof:* Let  $c_n/n^s$  be one of the terms of  $\zeta_{N,p,q}(s)$  with  $n = p^{e_1} q^{e_2}$ . Then

$$\begin{aligned} 1/n^s &= p^{-e_1 x} q^{-e_2 x} (\cos(\log(p^{e_1} q^{e_2})) + i \sin(\log(p^{e_1} q^{e_2}))) \\ &= p^{-e_1 x} q^{-e_2 x} (\cos((e_1 \log(p) + e_2 \log(q))y) \\ &\quad + i \sin((e_1 \log(p) + e_2 \log(q))y)). \end{aligned}$$

Using trigonometric summation formulas, we can express the real and imaginary parts of  $\zeta_{N,p,q}(s)$  as polynomials in  $p^{-x}, q^{-x}$  and the sine and cosine functions of  $(\log(p))y$  and  $(\log(q))y$ .

Let  $\gcd(m_1, m_2) = 1$ . Then we can find  $l_1, l_2 \in \mathbb{Z}$  with  $l_1 m_2 - l_2 m_1 = 1$ . Solving the linear system

$$\begin{aligned} (\log(q))y &= l_1 A + m_1 B, \\ (\log(p))y &= -l_2 A - m_2 B, \end{aligned}$$

in  $A$  and  $B$ , we obtain

$$\begin{aligned} A &= (m_1(\log(p)) + m_2(\log(q)))y, \\ B &= -(l_1(\log(p)) + l_2(\log(q)))y. \end{aligned}$$

Using trigonometric summation formulas again, we can express the real and imaginary parts of  $\zeta_{N,p,q}(s)$  as polynomials in  $p^{-x}, q^{-x}$  and the sine and cosine functions of  $A$  and  $B$ . Now we can use Gröbner basis reduction to eliminate  $\cos(B)$  and  $\sin(B)$  from the equations  $\Re(\zeta_{N,p,q}(s)) = 0$ ,  $\Im(\zeta_{N,p,q}(s)) = 0$ , and  $\cos^2(B) + \sin^2(B) = 0$ , obtaining a single equation  $F(x, \cos(A), \sin(A)) = 0$ . The zeros of  $\zeta_{N,p,q}(s)$  lie on this curve, which has period  $|2\pi i / (m_1(\log(p)) + m_2(\log(q)))|$  in  $y$ .  $\square$

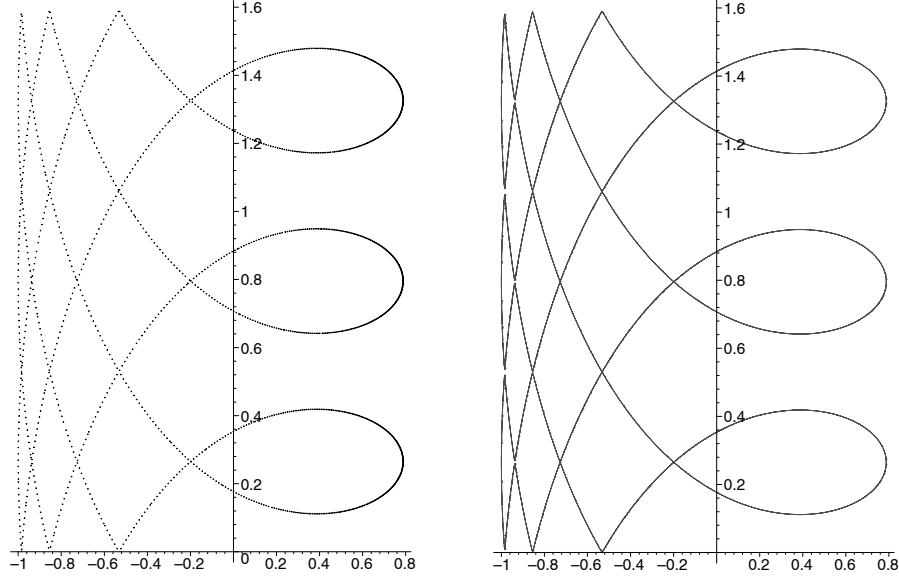


FIGURE 8. Zeros of  $\zeta_3(s)$  reduced modulo  $\frac{6\pi i}{\log(2^6 3^7)}$  and derived curve.

Here are some examples of the application of this theorem.

**Example 4.6.** On the left in Figure 8 we see zeros of  $\zeta_3(s)$  reduced modulo  $3 \left( \frac{2\pi i}{\log(2^6 3^7)} \right)$ .

We apply Theorem 4.5 with  $p = 2, q = 3, m_1 = 6, m_2 = 7$ , deriving  $l_1 = l_2 = 1$ . Then we have

$$\begin{aligned} (\log(2))y &= -A - 7B, \\ (\log(3))y &= A + 6B, \end{aligned}$$

where

$$A = (6 \log(2) + 7 \log(3))y, \quad B = -(\log(2) + \log(3))y.$$

Carrying out the algebraic reduction to remove the trigonometric terms in  $B$ , we obtain

$$\begin{aligned} &2 \cos(\log(2^6 3^7)y) \cdot 139968^{-x} + 4096^{-x} - 6 \cdot 43046721^{-x} \\ &- 153 \cdot 688747536^{-x} + 78 \cdot 502096953744^{-x} + 1287 \cdot 3869835264^{-x} \\ &- 405 \cdot 2754990144^{-x} - 825 \cdot 11019960576^{-x} + 21 \cdot 65536^{-x} \\ &- 21 \cdot 4194304^{-x} - 1287 \cdot 44079842304^{-x} + 252 \cdot 241864704^{-x} \\ &- 253 \cdot 55788550416^{-x} - 1254 \cdot 967458816^{-x} - 78 \cdot 339738624^{-x} \\ &- 825 \cdot 191102976^{-x} + 210 \cdot 1224440064^{-x} + 605 \cdot 24794911296^{-x} \\ &+ 715 \cdot 99179645184^{-x} + 462 \cdot 4897760256^{-x} + 462 \cdot 2176782336^{-x} \\ &+ 94 \cdot 1549681956^{-x} - 1716 \cdot 8707129344^{-x} + 1320 \cdot 429981696^{-x} \\ &- 715 \cdot 1719926784^{-x} + 59 \cdot 125524238436^{-x} \\ &+ 126 \cdot 26873856^{-x} + 7 \cdot 19131876^{-x} + 125 \cdot 589824^{-x} \\ &- 41 \cdot 172186884^{-x} - 71 \cdot 37748736^{-x} - 286 \cdot 223154201664^{-x} \\ &- 20 \cdot 3486784401^{-x} + 1716 \cdot 19591041024^{-x} - 750 \cdot 107495424^{-x} \\ &- 43 \cdot 147456^{-x} + 160 \cdot 9437184^{-x} + 855 \cdot 47775744^{-x} - 7 \cdot 16384^{-x} \end{aligned}$$

$$\begin{aligned} &- 67108864^{-x} - 35 \cdot 262144^{-x} + 13 \cdot 150994944^{-x} + 319 \cdot 84934656^{-x} \\ &+ 35 \cdot 1048576^{-x} + 6 \cdot 36864^{-x} + 2541865828329^{-x} \\ &- 6 \cdot 282429536481^{-x} + 7 \cdot 16777216^{-x} - 372 \cdot 11943936^{-x} \\ &- 13 \cdot 1129718145924^{-x} + 84 \cdot 306110016^{-x} - 190 \cdot 2359296^{-x} \\ &+ 396 \cdot 5308416^{-x} - 148 \cdot 1327104^{-x} - 106 \cdot 13947137604^{-x} \\ &- 510 \cdot 21233664^{-x} + 21 \cdot 331776^{-x} + 4782969^{-x} + 28 \cdot 76527504^{-x} \\ &+ 15 \cdot 387420489^{-x} + 300 \cdot 6198727824^{-x} + 286 \cdot 764411904^{-x} \\ &+ 15 \cdot 31381059609^{-x} + 56 \cdot 2985984^{-x} = 0, \end{aligned}$$

giving the plot on the right. This expression has 64 nonzero terms, with degrees 1 in  $\cos(\log(2^6 3^7)y)$ , and 26 in each of  $2^{-x}$  and  $3^{-x}$  for comparison with data for other curves given below.

**Example 4.7.** Figure 9 shows zeros of  $\eta_4$  reduced modulo  $\frac{2\pi i}{\log(2)}$  and modulo  $\frac{2\pi i}{\log(3)}$ .

For the first diagram, the zeros lie on the curve given by

$$\begin{aligned} &4^{-x+1} \cos^2(\log(2)y) + 2(2^{-x} - 8^{-x}) \cos(\log(2)y) \\ &- 3 \cdot 4^{-x} + 9^{-x} - 16^{-x} - 1 = 0. \end{aligned}$$

This splits into linear factors in  $\cos(\log(2))$ , one giving the loops to the left of  $y = 0$  and the other giving the loops to the right. For the second diagram, the curves are given by

$$\begin{aligned} &4 \cos^2(\log(3)y) \cdot 9^{-x} \\ &+ (4 \cdot 27^{-x} + 4 \cdot 3^{-x} - 6 \cdot 48^{-x} - 2 \cdot 12^{-x}) \cos(\log(3)y) \\ &+ 256^{-x} - 64^{-x} - 2 \cdot 144^{-x} - 36^{-x} + 81^{-x} - 4^{-x} \\ &+ 2 \cdot 9^{-x} - 4 \cdot 16^{-x} + 1 = 0. \end{aligned}$$

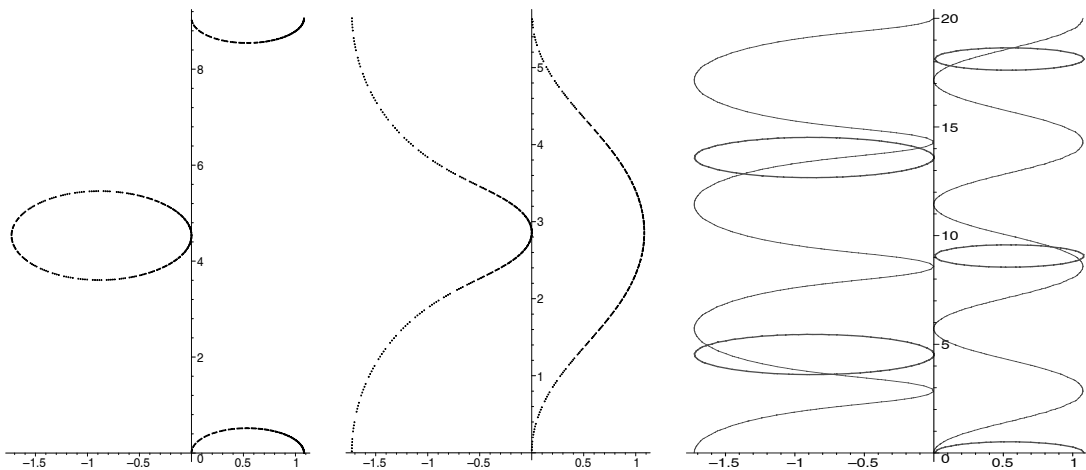


FIGURE 9. 500 zeros of  $\eta_4(s)$  reduced modulo  $\frac{2\pi i}{\log(2)}$ , modulo  $\frac{2\pi i}{\log(3)}$  and derived curves.

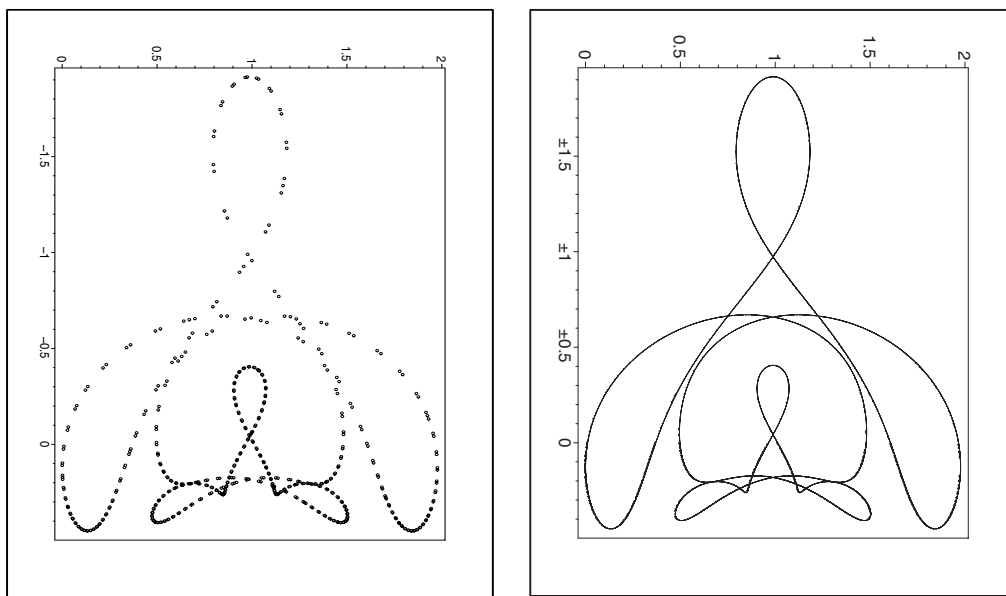


FIGURE 10. 506 zeros of  $\pi_{24}$  reduced modulo  $\frac{2\pi i}{\log(24)}$  and derived curve (Alexa's penguin).

This again splits, giving curves to the left and right of  $y = 0$ . The third plot shows several periods of these curves plotted together.

**Example 4.8.** We consider the function

$$\pi_{24}(s) := 1 + \frac{1}{2^s} + \frac{1}{3^s} + \frac{1}{4^s} + \frac{1}{6^s} + \frac{1}{8^s} + \frac{1}{9^s} + \frac{1}{12^s} + \frac{1}{16^s} + \frac{1}{18^s} + \frac{1}{24^s}.$$

Here the terms involve only the primes 2 and 3, so by Theorem 4.5 the zeros reduced modulo  $\frac{2\pi i}{\log(24)}$  will lie on a curve in the plane. Using the algebraic reduction

techniques outlined we derived an explicit formula for this curve, the data on which is contained in Table 1.

	no. of terms	$\deg(\cos(\log(24)y))$	$\deg(2^{-x})$	$\deg(3^{-x})$
$\pi_{24}$	1765	8	80	40

TABLE 1. Data of the curve of the reduced zeros of  $\pi_{24}$ .

Figure 10 depicts the curve. Notice that the picture is turned  $-90$  degrees to obtain a more dramatic effect.

#### 4.2 Multiple-Parameter Curves

We now examine the patterns that appear when the imaginary parts of the zeros of an exponential sum involv-

ing three or more primes are reduced via various periods. We start by reconsidering Figure 1 from the introduction, in which zeros of  $\zeta_5(s)$  are reduced modulo  $2\pi i/\log(5)$ . There no longer appears to be a simple curve. Since the number of zeros is countable, they cannot fill a region. However, there are areas where they appear to become dense. There are also shadings and outlines for curves that ask for explanation.

The zeros of  $\zeta(s)$  are the intersection points of the curves

$$1 + \frac{\cos(\log(2)y)}{2^x} + \frac{\cos(\log(3)y)}{3^x} + \frac{\cos(2\log(2)y)}{2^{2x}} \quad (4-7)$$

$$+ \frac{\cos(\log(5)y)}{5^x} = 0$$

and

$$\frac{\sin(\log(2)y)}{2^x} + \frac{\sin(\log(3)y)}{3^x} + \frac{\sin(2\log(2)y)}{2^{2x}} \quad (4-8)$$

$$+ \frac{\sin(\log(5)y)}{5^x} = 0.$$

We can eliminate the terms in  $\log(3)y$ , say, but we are still left with trigonometric terms in both  $\log(2)y$  and  $\log(5)y$ , so the function we obtain no longer has a simple period in  $y$  as before. We do note, however, that for values  $y_1 \pmod{2\pi/\log(2)}$ ,  $y_2 \pmod{2\pi/\log(3)}$ ,  $y_3 \pmod{2\pi/\log(5)}$ , we can find  $y$  such that the values  $y - y_1 \pmod{2\pi/\log(2)}$ ,  $y - y_2 \pmod{2\pi/\log(3)}$ ,  $y - y_3 \pmod{2\pi/\log(5)}$  are arbitrarily small. This leads us to consider  $\log(2)y$ ,  $\log(3)y$ , and  $\log(5)y$  as independent variables  $\log(2)y_1$ ,  $\log(3)y_2$ , and  $\log(5)y_3$ . The function

$$F(x, y_1, y_2, y_3) = 1 + 2^{x+iy_1} + 3^{x+iy_2} + 2^{2(x+iy_1)} \quad (4-9)$$

$$+ 5^{x+iy_3}$$

maps  $\mathbb{R}^4$  into  $\mathbb{C}$ . The zeros of  $F$  are not discrete, but lie on smooth surfaces. The function  $F$  is periodic in the variables  $y_1, y_2, y_3$  with periods  $\pi_1 = 2\pi/\log(2)$ ,  $\pi_2 = 2\pi/\log(3)$ ,  $\pi_3 = 2\pi/\log(5)$  respectively. Thus, the zeros of  $F$  in  $\mathbb{R} \times \prod_{j=1}^3 [0, \pi_j]$  may be taken as representatives of all the zeros of  $F$ . The partial diagonal map  $I : x + iy \rightarrow (x, y, y, y)$  takes  $\mathbb{C}$  into  $\mathbb{R}^4$ . We would like to investigate the relationship between the zeros of  $\zeta_5(s)$  via the map  $I$  and the zeros of  $F$ . We approach this more generally in the following theorem.

**Theorem 4.9.** *Let*

$$F(x, y_1, y_2, \dots, y_k) : \mathbb{R}^{k+1} \rightarrow \mathbb{C}$$

*be continuously differentiable and periodic in the variables  $y_1, y_2, \dots, y_k$  with periods  $\pi_1, \pi_2, \dots, \pi_k$ , which are*

*rationally independent. Let  $I : \mathbb{C} \rightarrow \mathbb{R}^{k+1}$  be the injection  $x + iy \rightarrow (x, y, y, \dots, y)$  and*

$$R : \mathbb{R}^{k+1} \rightarrow \mathbb{R} \times \prod_{j=1}^k [0, \pi_j]$$

*the reduction map taking each  $y_j$  to its equivalent modulus in the period  $[0, \pi_j]$ . Suppose that the function  $f(x+iy) = F(x, y, \dots, y) = F \circ I$  defines a complex analytic function and that  $\{(x, y_1, y_2, \dots, y_k) : \frac{\partial F}{\partial x} \neq 0\}$  is dense in  $\mathbb{R}^{k+1}$ . Then the zeros of  $f$  under the composition  $R \circ I$  are dense in the zeros of  $F$  in  $\mathbb{R} \times \prod_{j=1}^k [0, \pi_j]$ .*

*Proof:* Let  $X_z = (x, y_1, y_2, \dots, y_k) \in \mathbb{R} \times \prod_{j=1}^k [0, \pi_j]$  be a zero of  $F$ . We wish to show that for  $\varepsilon > 0$  we can find a zero  $z$  of  $f$  and a preimage  $\overline{X}_z \in R^{-1}(X_z)$  such that  $|I(z) - \overline{X}_z| < \varepsilon$ . By the hypothesis, we may restrict ourselves to  $X_z$  for which  $a = \frac{\partial F}{\partial x}(X_z) \neq 0$ . Certainly, we may find  $z$  and  $\overline{X} \in R^{-1}(X_z)$  such that  $I(z)$  and  $\overline{X}$  are as close as we like. The problem is to find such a  $z$  with  $f(z) = 0$ . We start by finding  $z_0$  and  $\overline{X}_z$  close enough and then show that the iterates

$$z_{n+1} = z_n - \frac{f(z_n)}{f'(z_n)}$$

obtained using Newton's method converge to the desired  $z$ .

Let  $\varepsilon > 0$  be given. By the continuity of the derivatives, we can find  $\delta_1 < \varepsilon$  such that

$$|X - X_z| < \delta_1 \Rightarrow \left| \frac{\partial F}{\partial x}(X) - a \right| < \frac{\min\{|a|, 1\}}{8(k+1)}.$$

Further, by continuity, we can find  $\delta_2 < \delta_1$  such that

$$|X - X_z| < \delta_2 \Rightarrow |F(X)| < \frac{\delta_1 |a|}{8(k+1)}.$$

We now find  $z_0 \in \mathbb{C}$  such that  $|I(z_0) - \overline{X}_z| < \delta_2/2$  for some  $\overline{X}_z \in R^{-1}(X_z)$ . We note the following:

- (1)  $f'(x + iy) = \frac{\partial f}{\partial x}(x + iy) = \frac{\partial F}{\partial x}(I(x + iy))$ .
- (2) If  $|I(z') - \overline{X}_z| < \delta_1$  and  $|I(z'') - \overline{X}_z| < \delta_1$  then  $\left| \frac{f(z'') - f(z')}{z'' - z'} \right| < \frac{\min\{|a|, 1\}}{8(k+1)}$ . Otherwise, for some point  $z'''$  on the line between  $z'$  and  $z''$ , we would have  $|f'(z''')| \geq \frac{\min\{|a|, 1\}}{8(k+1)}$ . However, since  $|I(z''') - \overline{X}_z| < \delta_1$ , this contradicts our choice for  $\delta_1$ .
- (3)  $|f'(z) - a| < |a|/8(k+1) \Rightarrow |f'(z)| \geq (8k+7)|a|/8(k+1)$ .

(4) In  $\mathbb{C}$ ,  $|z' - z''| < \delta/(k+1) \Rightarrow |I(z') - I(z'')| < \delta$   
in  $\mathbb{R}^{k+1}$ .

We now examine the Newton's method iterates. By the choice of  $\delta_2$  we have

$$\begin{aligned} |z_1 - z_0| &= \left| \frac{f(z_0)}{f'(z_0)} \right| = \left| \frac{f(z_0)}{a} + f(z_0) \left( \frac{1}{f'(z_0)} - \frac{1}{a} \right) \right| \\ &\leq \left| \frac{F \circ I(z_0)}{a} \right| + \left| \frac{F \circ I(z_0)}{a} \right| \left| \frac{F \circ I(z_0) - a}{(F \circ I)'(z_0)} \right| \\ &< \frac{\delta_1}{8(k+1)} + \frac{\delta_1}{8(k+1)} \frac{|a|}{8(k+1)} \frac{8(k+1)}{|a|(8k+7)} \\ &< \frac{\delta_1}{4(k+1)}. \end{aligned}$$

This implies  $|I(z_1) - I(z_0)| < \delta_1/4$  and ensures that  $|I(z_1) - \overline{X}_z| < 3\delta_1/4$ , so we still have control over the size of the derivative.

We assume inductively that  $|I(z_{n+1}) - \overline{X}_z| < \delta_1$  and  $|I(z_n) - \overline{X}_z| < \delta_1$ , which is true for  $n = 0$ . Then we have

$$\begin{aligned} \left| \frac{f(z_{n+1})}{z_{n+1} - z_n} \right| &= \left| \frac{f(z_{n+1}) - f(z_n)}{z_{n+1} - z_n} - f'(z_n) \right| \\ &\leq \left| \frac{f(z_{n+1}) - f(z_n)}{z_{n+1} - z_n} - a \right| + |a - f'(z_n)| \\ &< \frac{\min\{|a|, 1\}}{4(k+1)}, \end{aligned}$$

and then we have

$$\begin{aligned} |z_{n+2} - z_{n+1}| &= \left| \frac{f(z_{n+1})}{f'(z_{n+1})} \right| \\ &< \frac{\min\{|a|, 1\}}{4(k+1)} |z_{n+1} - z_n| \frac{8(k+1)}{|a|(8k+7)} \\ &< \frac{|z_{n+1} - z_n|}{2(k+1)}. \end{aligned}$$

This gives  $|I(z_{n+2}) - I(z_{n+1})| < \frac{1}{2}|I(z_{n+1}) - I(z_n)|$ , so we always have  $|I(z_n) - \overline{X}_z| < \delta_1$  as our Newton's method proceeds. The sequence  $z_n$  converges to some  $z \in \mathbb{C}$  with  $f(z) = F(I(z)) = 0$ . Also,  $|I(z) - \overline{X}_z| \leq \delta_1 < \varepsilon$ , as required.  $\square$

We apply this theorem along with Theorem 3.1 to establish a lower bound for the real parts of zeros of  $\zeta_N(s)$  for  $N$  prime.

**Theorem 4.10.** *For  $N$  prime we have*

$$\inf\{\sigma : \zeta_N(s) = 0\} = \beta_N,$$

where  $\beta_N$  is the negative root of  $\zeta_{N-1}(\beta_N) = N^{-\beta_N}$ .

*Proof:* Suppose that  $p_j$  is the  $j$ th prime with  $p_k = N$ . Substituting  $\log(p_j)t = y_j$  in the equations  $\Re((\zeta_N(s)) = 0$  and  $\Im((\zeta_N(s)) = 0$ , we obtain

$$\begin{aligned} 1 + 2^{-x} \cos(y_1) + 3^{-x} \cos(y_2) + \dots + N^{-x} \cos(y_k) &= 0, \\ 2^{-x} \sin(y_1) + 3^{-x} \sin(y_2) + \dots + N^{-x} \sin(y_k) &= 0. \end{aligned}$$

We see that the substitutions  $y_j = 0$  for  $1 \leq j \leq N-1$  and  $y_k = \pi$  cause the second equation to vanish and transform the first to

$$1 + 2^{-x} + 3^{-x} + \dots + (N-1)^{-x} - N^{-x} = 0,$$

for which the negative root is  $\beta_N$ . Applying Theorem 4.9, we can find roots of  $\zeta_N(\sigma + it)$  for which  $\sigma$  is arbitrarily close to  $\beta_N$ . Applying Theorem 3.1, the result follows.  $\square$

To relate Theorem 4.9 back to our diagrams, we use the projection  $P : \mathbb{R}^{k+1} \rightarrow \mathbb{C}$  defined by  $P(x, y_1, \dots, y_k) = x + iy_k$ . The next corollary follows directly.

**Corollary 4.11.** *Let  $F, f$  be as in Theorem 4.9 and let  $V$  be the zeros of  $F$  in  $\mathbb{R} \times \prod_{j=1}^k [0, \pi_j]$ . Then the zeros of  $f$  reduced into the period  $0 \leq y < \pi_k$  are dense in  $P(V)$ .*

We return to Figure 1 to illustrate Corollary 4.11. The zeros of  $\zeta_5(s)$  reduced modulo  $2\pi i/\log(5)$  are dense in the  $P$ -image of the zeros of  $F(x, y_1, y_2, y_3)$ , as defined in (4-9), in  $\mathbb{R} \times \prod_{j=1}^3 [0, \pi_j]$ . We can obtain equations for bounding curves by examining the extreme  $x$ -values of zeros of  $F$ . These zeros satisfy

$$\begin{aligned} F_r = 1 + \frac{\cos(\log(2)y_1)}{2^x} + \frac{\cos(\log(3)y_2)}{3^x} + \frac{\cos(2 \log(2)y_1)}{2^{2x}} \\ + \frac{\cos(\log(5)y_3)}{5^x} = 0 \end{aligned} \tag{4-10}$$

and

$$\begin{aligned} F_i = \frac{\sin(\log(2)y_1)}{2^x} + \frac{\sin(\log(3)y_2)}{3^x} + \frac{\sin(2 \log(2)y_1)}{2^{2x}} \\ + \frac{\sin(\log(5)y_3)}{5^x} = 0, \end{aligned} \tag{4-11}$$

where  $F_r$  and  $F_i$  are the real and imaginary parts of  $F$ . We regard (4-10) and (4-11) as defining  $x$  implicitly as a function of the independent variables  $y_1$  and  $y_3$ . To find the bounding curve of the image in  $\mathbb{C}$  of the zeros of  $F$ , we find the extreme values of  $x$  for each fixed  $y_3$  by setting  $\frac{\partial x}{\partial y_1} = 0$ .

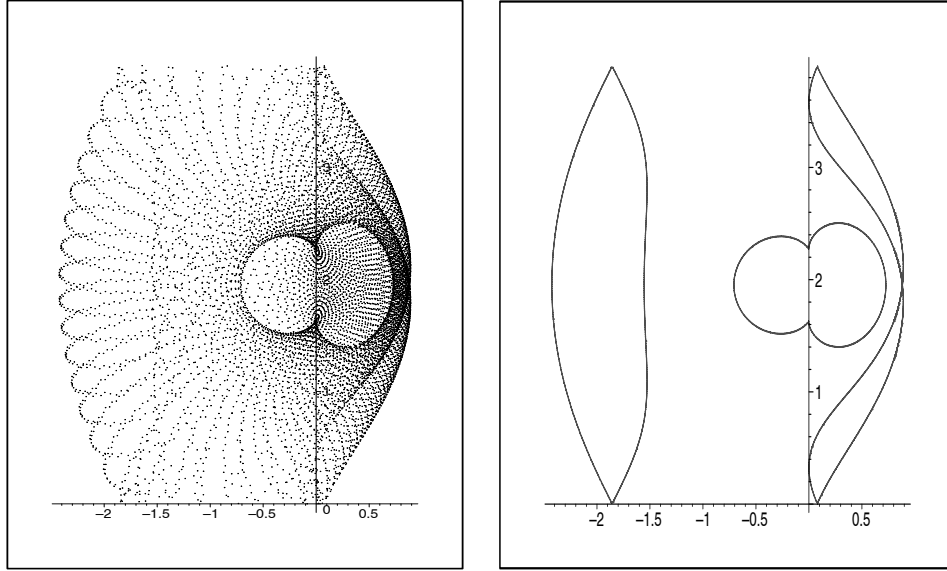


FIGURE 11. Zeros of  $\zeta_5(s)$  reduced modulo  $\frac{2\pi i}{\log(5)}$  with bounding curve.

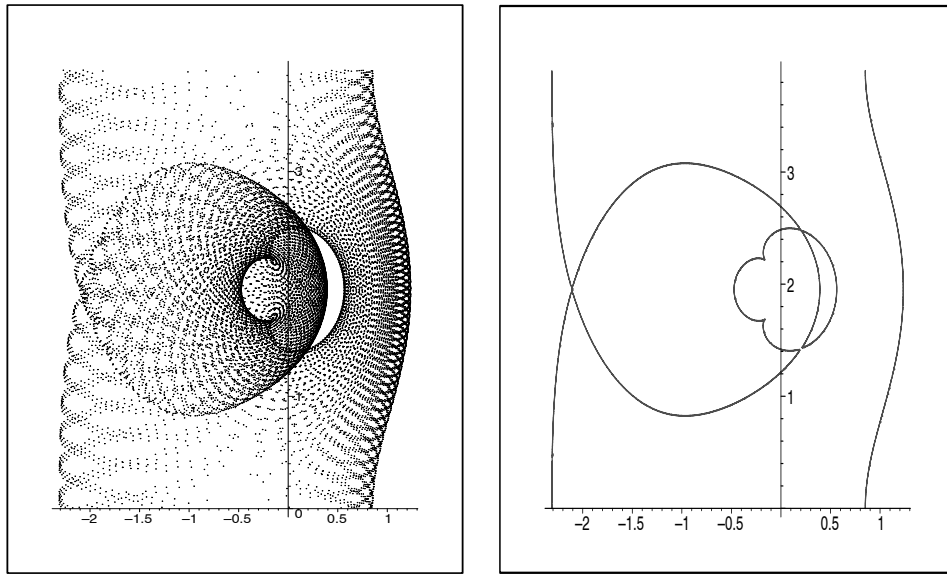


FIGURE 12. 10,000 zeros of  $\eta_5(s)$  reduced modulo  $\frac{2\pi i}{\log(5)}$  with bounding curve.

Taking partial derivatives of (4-10) and (4-11) with respect to  $y_1$ , we obtain

$$\begin{aligned} \frac{\partial F_r}{\partial x} \frac{\partial x}{\partial y_1} + \frac{\partial F_r}{\partial y_1} + \frac{\partial F_r}{\partial y_2} \frac{\partial y_2}{\partial y_1} &= 0, \\ \frac{\partial F_i}{\partial x} \frac{\partial x}{\partial y_1} + \frac{\partial F_i}{\partial y_1} + \frac{\partial F_i}{\partial y_2} \frac{\partial y_2}{\partial y_1} &= 0. \end{aligned}$$

We then eliminate  $\frac{\partial y_2}{\partial y_1}$  to obtain the condition

$$\frac{\partial F_r}{\partial y_1} \frac{\partial F_i}{\partial y_2} - \frac{\partial F_r}{\partial y_2} \frac{\partial F_i}{\partial y_1} = 0.$$

Note that regarding  $y_1$  as the dependent variable and  $y_2$  independent leads to the same condition.

Doing the formal differentiation, we obtain the equation

$$\begin{aligned} &\frac{\sin(\log(3)y_2)}{3^x} \left( \frac{\cos(\log(2)y_1)}{2^x} + \frac{2 \cos(2 \log(2)y_1)}{2^{2x}} \right) \\ &- \frac{\cos(\log(3)y_2)}{3^x} \left( \frac{\sin(\log(2)y_1)}{2^x} + \frac{2 \sin(2 \log(2)y_1)}{2^{2x}} \right) \\ &= 0. \end{aligned} \tag{4-12}$$

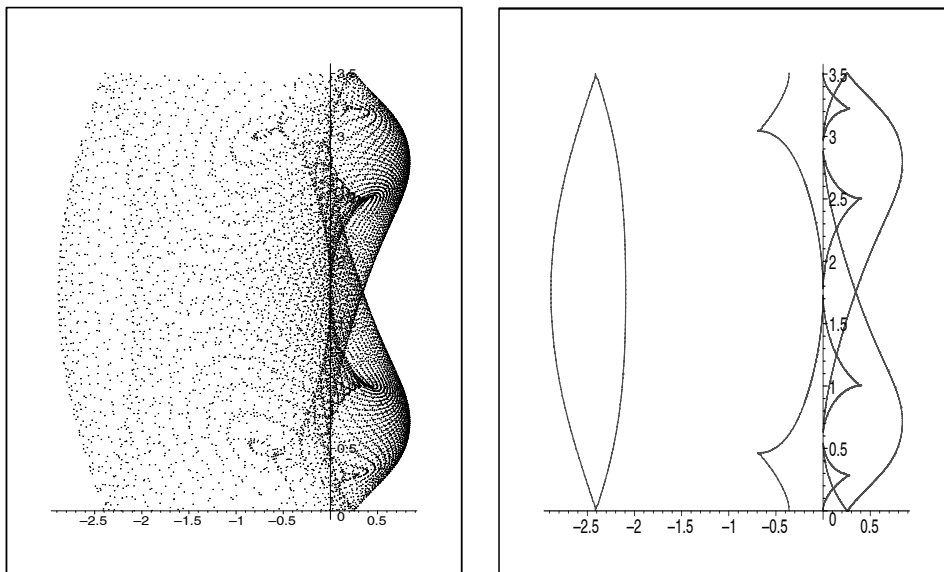


FIGURE 13. 12,000 zeros of  $\zeta_6(s)$  reduced modulo  $\frac{2\pi i}{\log(6)}$  with bounding curve.

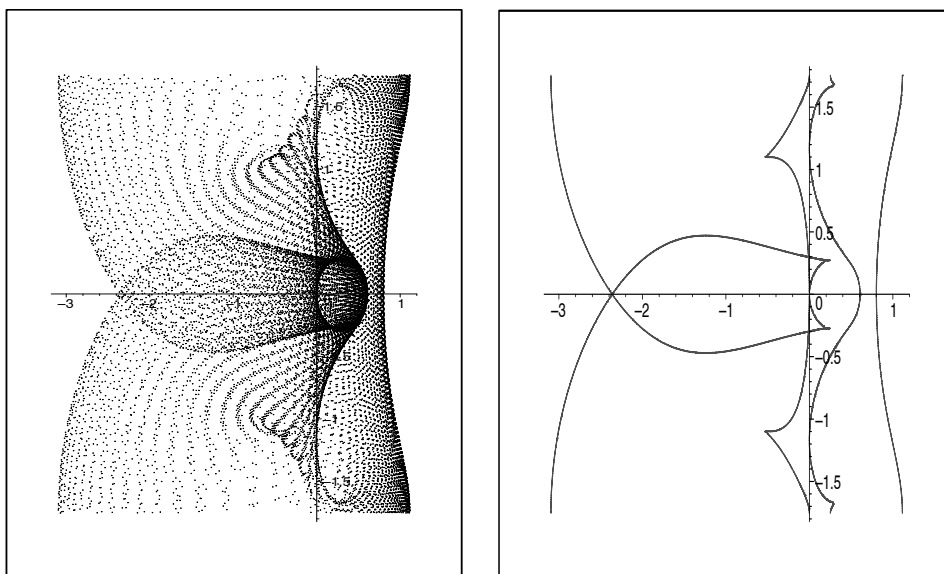


FIGURE 14. 12,000 zeros of  $\eta_6(s)$  reduced modulo  $\frac{2\pi i}{\log(6)}$  and bounding curve.

We now have the three Equations (4–10), (4–11), and (4–12) to describe the bounding curve. Using algebraic reduction we can eliminate terms in  $\log(2)y_1$  and  $\log(3)y_2$  to obtain a single equation involving  $x$  and  $\log(5)y_3$  having period  $2\pi i/\log(5)$ .

In Figure 11 we see the comparison between reduced zeros of  $\zeta_5(s)$  and a plot of the image of the curve given by this equation under the projection  $P$ .

Applying the same technique, we can derive the equation for the bounding curve for the zeros of  $\eta_5(s)$  reduced modulo  $2\pi i/\log(5)$ . These are illustrated in Figure 12. Of interest here is the crescent-moon-shaped area that appears to exclude zeros. Data on the equations derived for these bounding curves is given in Table 2.

The algebraic reduction entailed is already fairly involved. For  $\zeta_6(s)$  (Figure 13) and  $\eta_6(s)$  (Figure 14) the

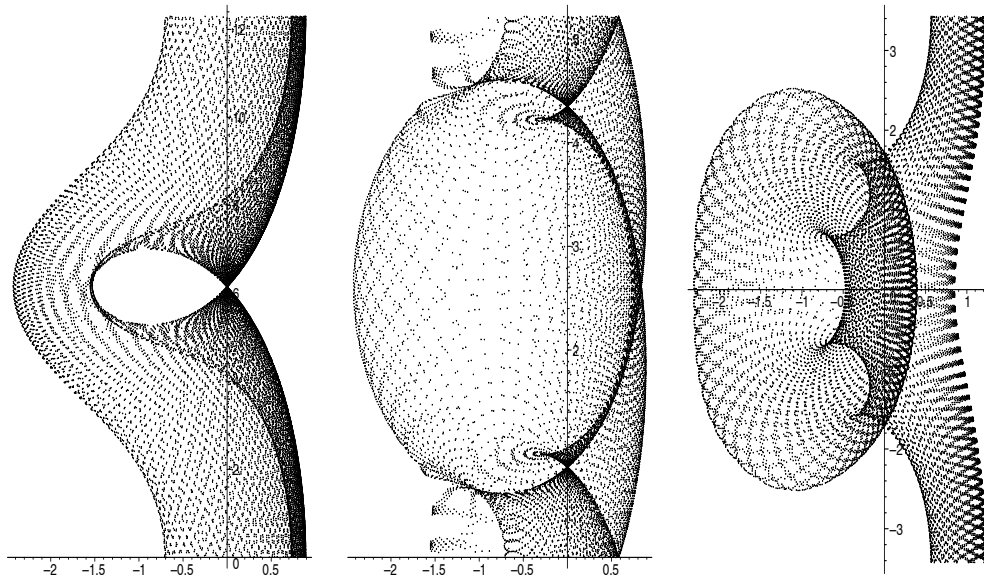


FIGURE 15. 20,000 zeros of  $\zeta_5(s)$  reduced modulo  $\frac{2\pi i}{\log(5/3)}$  (left) and  $\frac{2\pi i}{\log(10/3)}$  (center). 20,000 zeros of  $\eta_5(s)$  reduced modulo  $\frac{2\pi i}{\log(5/2)}$  (right).

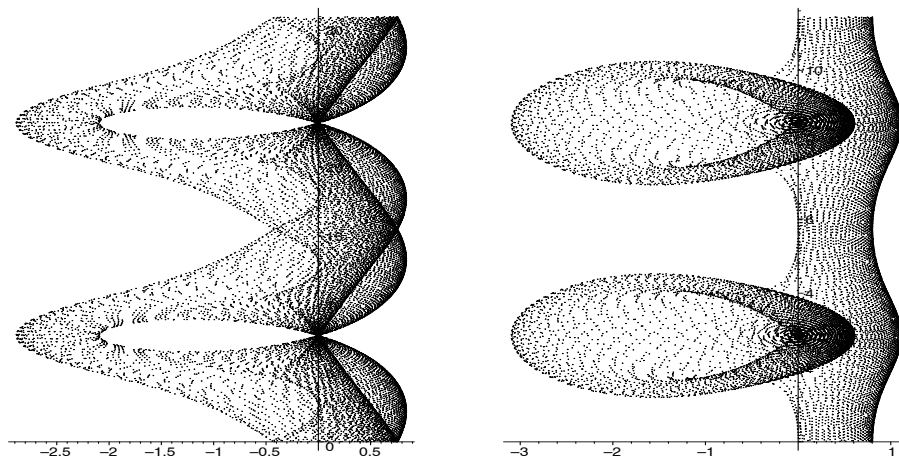


FIGURE 16. 20,000 zeros of  $\zeta_6(s)$  and  $\eta_6(s)$  reduced modulo  $\frac{4\pi i}{\log(3/2)}$  and  $\frac{4\pi i}{\log(3)}$ , respectively.

	no. of terms	$\deg(\cos(\log(5)y))$	$\deg(2^{-x})$	$\deg(3^{-x})$	$\deg(5^{-x})$
$\zeta_5$	183	5	16	8	10
$\eta_5$	185	5	16	8	10

TABLE 2. Data of the bounding curves of  $\zeta_5$  and  $\eta_5$ .

data on the equations for the bounding curves are given in Table 3. These evaluations were done using Maple 8, and seem to approach the limit of what current algebraic packages are able to handle practically.

For these examples, what are probably the more obvious periods, i.e.,  $2\pi i/\log(N)$ , were chosen for reducing zeros. As in the case with two prime exponential sums, we can choose a period  $2\pi i/L$ , where  $L$  is a rational lin-

ear combination of  $\log(p_j)$ 's for primes  $p_j$  appearing in the sum. The finer structures of these diagrams are more apparent in the sums involving three primes; see Figures 15 and 16. With more primes, the diagrams for some periods often seem fairly amorphous. However, as we see in Figure 17, the choice of an appropriate period may still give a diagram with interesting separations of points.

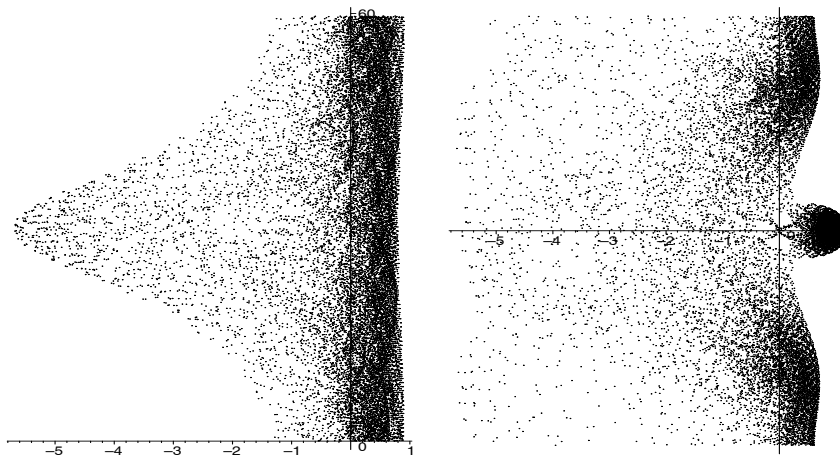


FIGURE 17. 20,000 zeros of  $\zeta_{10}(s)$  and  $\eta_{10}(s)$  reduced modulo  $\frac{2\pi i}{\log(10/9)}$  and  $\frac{2\pi i}{\log(2)}$ , respectively.

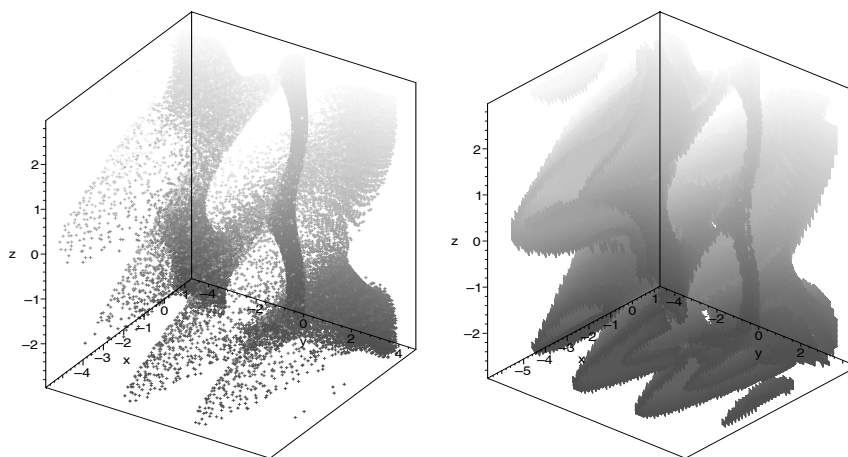


FIGURE 18. 50,000 zeros of  $\eta_{10}(s)$  reduced into  $\mathbb{R} \times \left[ \frac{-\pi}{\log(2)}, \frac{\pi}{\log(2)} \right] \times \left[ \frac{-\pi}{\log(3)}, \frac{\pi}{\log(3)} \right]$  and bounding surface.

	no. of terms	$\deg(\cos(\log(6)y))$	$\deg(2^{-x})$	$\deg(3^{-x})$	$\deg(5^{-x})$
$\zeta_6$	1197	7	30	18	12
$\eta_6$	1202	7	30	18	12

TABLE 3. Data of the bounding curves of  $\zeta_5$  and  $\eta_6$ .

### 5. FURTHER WORK

A natural extension is to look at projections into more than one period, giving representations of zeros in higher-dimensional spaces. For  $\zeta_5$ , for example, and other Dirichlet series involving three primes, an appropriate 3D representation in  $\mathbb{R} \times [0, \pi_1] \times [0, \pi_2]$ , for appropriate periods  $\pi_1, \pi_2$ , will show the reduced zeros becoming dense in a surface. Figure 18 shows a further rendering of zeros of  $\eta_{10}$ , where the  $x$ -axis represents the real part, the  $y$ -axis the residue of the imaginary part in the period

$\left[ \frac{-\pi}{\log(2)}, \frac{\pi}{\log(2)} \right]$ , and the  $z$ -axis the residue of the imaginary part in the period  $\left[ \frac{-\pi}{\log(3)}, \frac{\pi}{\log(3)} \right]$ . This gives more detail than the 2D rendering in the right of Figure 17, which is the view through the bottom of the box. The rounded bump shown on the right in Figure 17 is shown to extend in a ropelike structure along the  $z$ -axis. The somewhat amorphous scattering of zeros seen on the right resolves into ridges running diagonally in the  $yz$ -plane. The graphic on the right shows the bounding surface for the zeros. This parametric equation was obtained using

differentiation and algebraic reduction as described in the previous section.

Further work planned includes the extension of work of van de Lune and te Riele [van de Lune and te Riele 82] to find near extreme zeros of partial sums of the  $\zeta$ -function, in particular, zeros with real part greater than 1. Also, we would like to extend this investigation to include partial sums of  $L$ -series.

## ACKNOWLEDGMENTS

Research for all of the authors was supported by MITACS of Canada. Research of P. Borwein was supported as well by NSERC of Canada. Research of A. van der Waall was supported as well by the Netherlands Organization for Scientific Research (NWO), travel fund file number R 61-504. We thank Nils Bruin of the University of Sydney for conducting the extended calculation to derive the equation of the curve shown in Figure 10 using the computer algebra system Magma [Bosma et al. 97].

## REFERENCES

- [Bosma et al. 97] Wieb Bosma, John Cannon, and Catherine Playoust. “The Magma Algebra System I: The User Language.” *J. Symbolic Comput.* 24:3–4 (1997), 235–265.
- [Conrey 03] J. Brian Conrey. “The Riemann Hypothesis.” *Notices Amer. Math. Soc.* 50:3 (2003), 341–353.
- [Conrey 89] J. B. Conrey. “More Than Two Fifths of the Zeros of the Riemann Zeta Function Are on the Critical Line.” *J. Reine Angew. Math.* 399 (1989) 1–26.
- [Edwards 01] H. M. Edwards. *Riemann’s Zeta Function*. Mineola, NY: Dover Publications Inc., 2001. Reprint of the 1974 original, New York: Academic Press.
- [Jentzsch 18] R. Jentzsch. “Untersuchungen zur Theorie der Folgen analytischer Functionen.” *Acta Math.* 41 (1918), 219–251.
- [Langer 31] R. E. Langer. “On the Zeros of Exponential Sums and Integrals.” *Bull. Amer. Math. Soc.* 37 (1931), 213–239.
- [van de Lune and te Riele 82] J. van de Lune and H. J. J. te Riele. “Numerical Computation of Special Zeros of Partial Sums of Riemann’s Zeta Function.” In *Computational Methods in Number Theory, Part II*, pp. 371–387, Math. Centre Tracts 155. Amsterdam: Math. Centrum, 1982.
- [Montgomery 83] H. L. Montgomery. “Zeros of Approximations to the Zeta Function.” In *Studies in Pure Mathematics*, pp. 497–506. Basel: Birkhäuser, 1983.
- [Patterson 88] S. J. Patterson. *An Introduction to the Theory of the Riemann Zeta Function*. Cambridge: Cambridge University Press, 1988.
- [Spira 66] Robert Spira. “Zeros of Sections of the Zeta Function I.” *Math. Comp.* 20 (1966), 542–550.
- [Titchmarsh 86] E. C. Titchmarsh. *The Theory of the Riemann Zeta Function*, Second edition. New York: Oxford University Press, 1986.
- [Turán 48] P. Turán. “On Some Approximative Dirichlet-Polynomials in the Theory of the Zeta Function of Riemann.” *Danske Vid. Selsk. Mat.-Fys. Medd.* 24:17 (1948), 36.
- [Turán 59] P. Turán. “Nachtrag zu meiner Abhandlung ‘On Some Approximative Dirichlet Polynomials in the Theory of the Zeta Function of Riemann.’” *Acta Math. Acad. Sci. Hungar.* 10 (1959) 277–298 (unbound insert).
- [Wilder 17] Charles E. Wilder. “Expansion Problems of Ordinary Linear Differential Equations with Auxiliary Conditions at More Than Two Points.” *Trans. Amer. Math. Soc.* 18:4 (1917), 415–442.

Peter Borwein, Department of Mathematics, Simon Fraser University, Burnaby, British Columbia, Canada V5A 1S6  
(pborwein@cecm.sfu.ca)

Greg Fee, Department of Mathematics, Simon Fraser University, Burnaby, British Columbia, Canada V5A 1S6  
(gfee@cecm.sfu.ca)

Ron Ferguson, Department of Mathematics, Simon Fraser University, Burnaby, British Columbia, Canada V5A 1S6  
(rferguson@pims.math.ca)

Alexa van der Waall, Department of Mathematics, Simon Fraser University, Burnaby, British Columbia, Canada V5A 1S6  
(awaall@cecm.sfu.ca)

Received June 27, 2005; accepted August 9, 2005.

